Correlation of an Alcohol's αC−D Stretch with Hydrogen Bond Strength in Complexes with Amines

Nakul C. Maiti, Paul R. Carey, and Vernon E. Anderson*

Departments of Biochemistry and Chemistry, Case Western Reserve University, 10900 Euclid Avenue, Cleveland, Ohio 44106-4935

Received: April 8, 2003; In Final Form: August 12, 2003

The enthalpies of H-bond formation between 1,1,1,3,3,3-hexafluoro-2-propanol (HFIP) as donor and tertiary amines of varying pK_a's as acceptors were determined by isothermal calorimetry. The stretching frequencies of the αC−D of HFIP-d_2 in dilute solution and in different H-bonded amine solvents were measured by Raman spectroscopy. Dilute HFIP-d_2 in chloroform showed two C−D stretching features at 2195 and 2168 cm^{-1} which are assigned to the anti and gauche conformations of the molecule on the basis of precedent and theoretical calculations. The molecular structure, relative energies, and C−D stretching frequency (ν_{C-D}) of the anti and gauche conformations of HFIP and HFIP-d_2 and their H-bonded complexes with trimethylamine were calculated by density functional theory using a B3LYP/6-31+G(d,p) basis set. In the monomeric state, the calculated ν_{C-D} for the gauche conformation was 52 cm^{-1} lower than the anti conformations. Both ν_{C-D} bands were red-shifted when the O−H(D) group functioned as a H-bond donor with amine receptors. Among the different tertiary amines, the alcohol forms the weakest H bond with *N*,*N*-dimethylaniline and the strongest bond with quinuclidine. The enthalpy of H-bond formation and the gauche and anti αC−D, stretching frequencies were correlated, having slopes of -2 ± 1 and -4 ± 1.5 cm^{-1}/(kcal mol^{-1}), respectively. The results indicate increasing H-bond strength results in an increase in negative hyperconjugation of the vicinal C−D bond. Observation of ν_{C-D} of specifically labeled (HO)C−D groups can be used to provide a spectroscopic characterization of a specific H bond present in macromolecular complexes when the OH group is bound to a single H-bond acceptor.

Introduction

H-bonds have been recognized as playing a fundamental role in the determination of the structure and function of proteins and nucleic acids. The complementary donor−acceptor nature of H-bonds along with the geometric constraints of distance and angle required for the formation of H-bonds are characteristics that generate much of the specificity encountered in molecular recognition and enzyme catalysis.[1] Model compounds have been employed to understand the energetics of enzyme−substrate and receptor−ligand binding interactions.[2] In molecular biological studies, it is common to selectively alter the structure of the ligand or the protein by site-directed mutagenesis to eliminate a H-bond. The difference in affinity has been interpreted as the strength of the individual H-bond, but this neglects the effects of solvation and the perturbation of the system introduced by the chemical or genetic manipulation, which invariably leads to changes in conformation and/or solvation that are accompanied by both enthalpic and entropic effects.

Spectroscopic methods are being developed to determine individual H-bond strengths. In small molecule crystals, the H-bonding distance between the donor and acceptor heteroatoms correlates well with O−H stretching frequency, and presumably H-bond strength.[3,4] For macromolecular complexes, H-bond lengths can be measured in single crystals. However, this approach is limited by the difficulties involved in crystallization and refinement to a high enough resolution to permit confidence in the accuracy of the reported H-bonding distances. NMR measurements have the potential to characterize H-bonds from amide donors where the chemical shift, coupling constant, fractionation factor, and solvent exchange rate all are affected by H-bond strength.[1,5]

In aqueous solution, H-bonds from alcohol donors have been less amenable to spectroscopic characterization, largely because of the difficulty in differentiating the −OH group of interest from the broad and intense solvent background from H_2O. Vibrational spectroscopy has been used extensively to characterize H-bonds in nonaqueous solvents. The most direct characterization has been to monitor the O−H stretching frequency in the vibrational spectra of the H-bonded, O−H···B complex.[1,6] The correlation of the O−H frequency with H-bond strength was developed by comparing frequencies with calorimetric heats of formation.[7] Because of the broad, intense O−H band in water, this approach fails when attempting to identify specific O−H···B bonds in macromolecular complexes. Labeling a specific group with D is prevented by the rapid exchange of all O−H protons with solvent, and labeling with ^{18}O does not perturb the frequency sufficiently to differentiate the ^{18}O−H stretch from the intense water modes. NMR techniques have been of limited success because of the rapid solvent exchange of the OH group.

H-bond strengths to substrate carbonyl groups in serine proteases were previously characterized by determining the change of the carbonyl C═O stretching frequency.[8,9] The calibration from carbonyl frequency to H-bond strength was de-

* To whom correspondence should be addressed. E-mail: vea@cwru.edu. Phone: (216) 368-2599. Fax (216) 368-3419.

10.1021/jp0349334 CCC: $25.00
Published on Web 10/29/2003

SCHEME 1: Gauche and Anti Conformers of HFIP-d_2

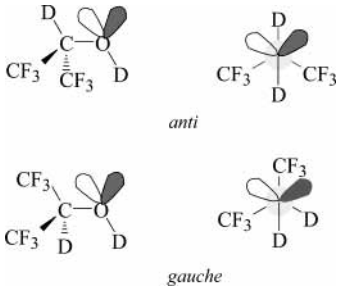

veloped by correlating Van't Hoff enthalpies of formation with the observed decreases in the C═O stretching frequency that characterized the H-bond.[8,9] This approach was successful because the carbonyl stretching frequency of the substrate was intensity enhanced by the resonance Raman effect.

A window in the Raman spectra of enzyme−substrate complexes exists in the region of the C−D stretch (ν_{C-D}), ca. 2250−2000 cm^{-1}. The unusual frequency for ν_{C-D} minimizes coupling to other vibrational modes and, because of the differences in masses, is easily interpreted as an isolated group frequency. Callender and co-workers[10] were able to identify individual C−D stretches of [4-D]NADH bound to lactate dehydrogenase by Raman difference spectroscopy indicating that the Raman cross section of a single C−D bond is sufficient to detect in enzyme substrate complexes. There is computational evidence that ν_{C-D} from D-labeled primary and secondary alcohols should be correlated with the strength of the H-bonds to and from the alcohol functionality.[11] Consequently, experimental characterization of the ν_{C-D} vibration of α-D alcohols will provide the groundwork for future studies of H-bonded complexes.

1,1,1,3,3,3-Hexafluoro-2-propanol (HFIP), by virtue of being a stronger acid, can form stronger H bonds than other alcohols, and the symmetry minimizes the number of conformers present in solution. The Raman and infrared spectra of HFIP and HFIP-d_2 have been previously characterized.[12−15] Both the ν_{O-H} and ν_{C-D} bands are doublets attributed to the presence of gauche and anti conformers defined about the (D)H−C−O−H(D) torsion angle (Scheme 1). The ν_{C-D} is of particular interest in this study as a potential reporter of H-bonding interactions of the O−H. In carbon tetrachloride, the gauche and anti ν_{C-D} stretches are assigned to bands at 2188 and 2165 cm^{-1}, respectively, based on symmetry and relative intensities. The observation of doublets for the α ν_{C-D} of mono deuterated alcohols is universal and was attributed to the anti and gauche conformers by Krueger et al.[16] Overlap of the O lone pair of electrons with the σ^* orbital of an anti C−D bond results in negative hyperconjugation and a decrease in the C−D frequency of as much as 60 cm^{-1}. These spectral assignments were corroborated by a recent gas phase study of HFIP and density function theory calculation.[17]

In a previous computational study, it was suggested that having the OH group act as an H-bond donor would enhance negative hyperconjugation in primary and secondary alcohols.[11] The formation of an H-bond delocalizes the electrons in the O−H σ bond resulting in an increased overlap with the antibonding orbital of the anti C−H bond (Scheme 2). This increased overlap reduces the αC−H bond order and produces a concomitant red shift in the vibrational frequency. In the present work, the Raman spectra of HFIP-d_2 H-bonded with tertiary amines of varying basicity have been obtained to test the computational prediction. The results demonstrate that H-bond formation is correlated with a decrease in ν_{C-D} of both

SCHEME 2: Lowest Unoccupied MO+1 of HFIP Calculated at the 6-31+G(d,p) Level, Effectively the C−H Antibonding Orbital

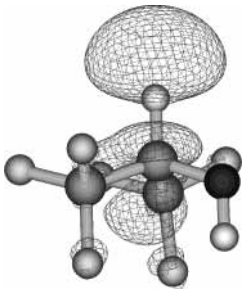

the gauche and anti conformers and that monitoring ν_{C-D} by Raman spectroscopy will provide a means of characterizing individual alcohol H bonds in macromolecular complexes.

Materials and Methods

HFIP and HFIP-d_2 were obtained from Aldrich. Other solvents were also obtained from Aldrich or Fisher Chemicals and used with out further purification.

Raman Spectroscopy. Raman spectra were obtained using 647.1 nm laser excitation from an Innova 400 krypton laser system (Coherent, Inc.), a back-illuminated charge-coupled device (CCD) detector (model 1024EHRB/1, Princeton Instruments, Inc.) operating at 183 K, and a Holospec f/1.4 axial transmission spectrometer (Kaiser Optical Systems, Inc.) employed as a single monochromator, as described previously.[18] The Raman spectra of HFIP/HFIP-d_2 were acquired as neat liquid and after dilution into other solvents. In one set of experiments, 0.5 M solutions of tertiary amines were prepared in chloroform and to each solution HFIP-d_2 (final concentration 20 mM) was added to form hydrogen bonded complexes. The sample (60 μL) was held in a 2 × 2 mm quartz cuvette under the 90° excitation/collection geometry, and the Raman spectra were collected using a laser power of ∼150 mW and CCD exposure times of 1 min. For each spectrum, generally 10 exposures were acquired. The Raman spectrum of the solvent was recorded for an equal time and subtracted from that of the alcohol−amine complexes. The solvent band was used as the normalization standard. The subtracted spectrum was baseline corrected by multi-point selection. Wavenumber calibration was performed by recording the Raman spectra of 1:1 mixture of cyclohexanone and acetone-d_6, providing band positions to within ±1 cm^{-1} for sharp bands. Data analysis was carried out using GRAMS/32 software (Galactic Industries, Inc.)

The band fitting of the Raman band profile of the ν_{C-D} features was done using the CurveFit.Ab nonlinear least squares routine in GRAMS/32. The AutoFind peak picker provided the initial number of peaks and their positions. The component bands were determined by curve fitting the spectra using Lorentzian bands.

Isothermal Titration Calorimetry. The enthalpy of H-bond formation was measured at 24 °C by using a MCS−ITC instrument from Micro Cal (Northampton, MA). In each experiment, 5−20 mM HFIP in chloroform was placed in the 1.4 mL sample cell. In all cases, the reference cell contained chloroform. Amine solutions in chloroform were added to the HFIP solution in the cell by means of a 500 μL syringe. The amine concentration was in the range of 50−200 mM. The solution in the sample cell was stirred continuously during the entire experiment at 300 rpm. Data were evaluated using the

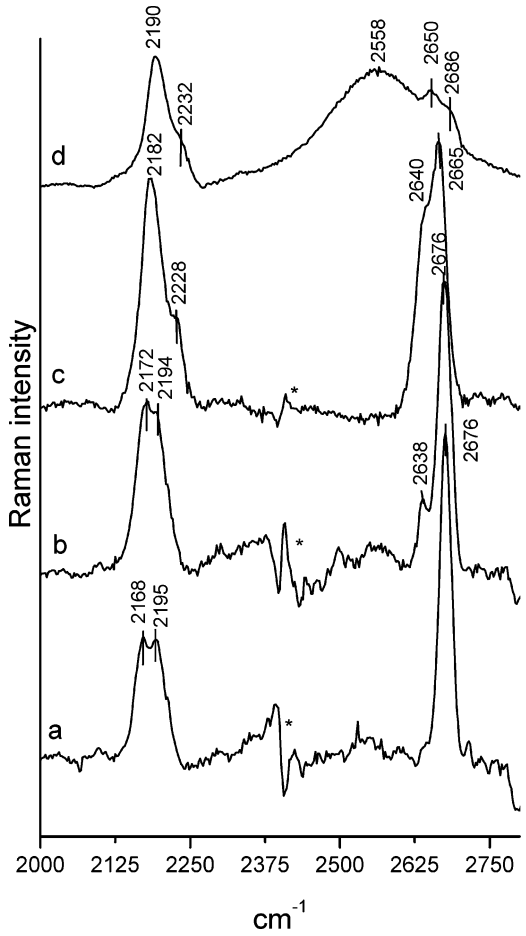

Figure 1. C−D and O−D stretching regions of the room-temperature Raman spectra of HFIP-d_2 at varying concentrations in chloroform. (a) 20 mM HFIP-d_2, (b) 0.1 M HFIP-d_2, (c) 1 M HFIP-d_2, and (d) neat HFIP-d_2.

ORIGIN 2.7 software supplied by the instrument manufacturer which determines both the enthalpy of interaction, the equilibrium constant and the heat of dilution for the titrant.

Results

The Raman spectrum of a dilute solution of HFIP-d_2 (20 mM) in chloroform in the ν_{C-D} region exhibits two bands of similar intensity at 2168 and 2195 cm^{-1} as shown in Figures 1 and 2. These two peaks are assigned to ν_{C-D} for the gauche and anti conformations of HFIP-d_2, respectively.[12−15] Figure 2 shows the band fitting of the C−D stretching region of the Raman spectrum of HFIP-d_2 in chloroform. Neat HFIP-d_2 has C−D vibration bands at 2190 and 2232 cm^{-1}. Band fitting reveals that the 2190 cm^{-1} feature has contributions from bands at 2187 and 2199 cm^{-1}, assigned to the gauche and anti conformations, respectively, and the band at 2232 cm^{-1}, based on its concentration dependence, is assigned to ν_{C-D} in aggregated HFIP-d_2. In neat HFIP-d_2, the O−D stretching region contains three overlapping bands at 2686, 2650, and 2558 cm^{-1} (Figure 1). The very broad band at 2558 cm^{-1} is assigned to the H-bonded O−D stretching vibrations present in the associated HFIP-d_2. The other two bands may be due to the O−D bands for the monomer and other smaller associated aggregates with both gauche and anti conformations present. In dilute chloroform solution, two OD fundamental vibrations appear at 2676 and 2687 cm^{-1} (the bands are overlapped and could be seen by expansion of the spectra). The two vibrational modes are assigned to the two conformations (anti and gauche, respectively) of monomeric HFIP-d_2.

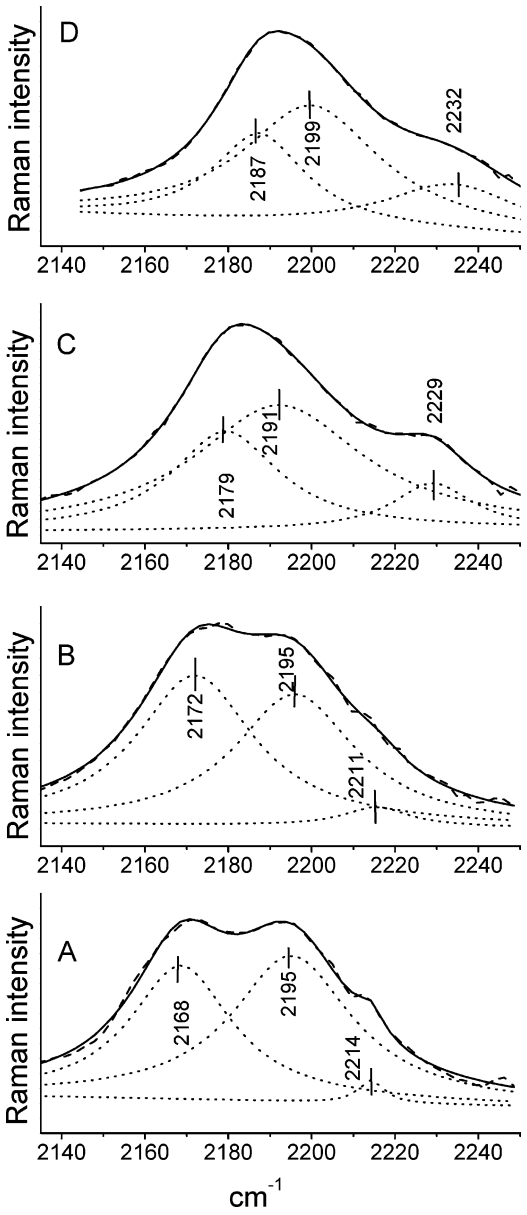

Figure 2. Band fitting of the C−D stretching region in the Raman spectra of HFIP-d_2 in $CHCl_3$. Experimental conditions were as in Figure 1. The peak positions of the component bands were determined by curve fitting the spectra assuming a linear combination of Lorentzian peaks. The dotted lines denote individual components, and the dashed lines the summation. The solid lines represent the experimentally determined spectra. (A) 20 mM HFIP-d_2, (B) 0.1 M HFIP-d_2, (C) 1 M HFIP-d_2, and (D) neat HFIP-d_2.

Raman spectra of HFIP-d_2 were recorded in other solvents to test the dependence of ν_{C-D} on solvent dielectric; the positions of both ν_{C-D} features are listed in Table 1.

Figure 3 shows the Raman spectra (ν_{C-D} region) of HFIP-d_2 in the amine solvents. Different tertiary amines of varying pK_a were used. The ν_{C-D} features were red-shifted to lower frequency in the amine solvents. For *N*,*N*-dimethylaniline, the anti and gauche conformational bands are resolved sufficiently to permit identification at 2187 and 2160 cm^{-1}, respectively (Figure 3A). The bands are red-shifted further in the presence of stronger bases, e.g., appearing at 2167 and 2154 cm^{-1} in triethylamine (pK_a = 11.2) (Figure 3D). For amines of intermediate basicity, the band profiles are shown in Figure 3 and reported in Table 2. As in neat HFIP-d_2, weak bands appear at higher frequency, at 2214 cm^{-1} in *N*,*N*-dimethylaniline and

TABLE 1: O−D and C−D Stretching Bands of HFIP-d_2 in a Number of Solvents

				ν_{C-D} (cm^{-1})				ν_{O-D} (cm^{-1})		
solvent	ϵ (D)	[HFIP-d_2] mM	pK_a	gauche	anti	dimer or aggregate	ion-pair	gauche	anti	dimer or aggregate
HFIP-d_2		neat	9.3	2187	2199	2232			2686	2650 2558
chloroform	3.7	10−500		2168	2195	2214		2676	2787	2640
CCl_4		10		2170	2196			2673	2695	2645
toluene	2.0	10		2168	2188			2679	2697	2630
N,*N*-dimethylaniline		67	6.6	2160	2187					
N-methyl morpholine		49	7.67	2159	2174	2212	2105			
N,*N*-diisopropylethylamine		49	∼11.0	2159	2174		2105			
triethylamine	2.44	113	10.8	2154	2167		2105			

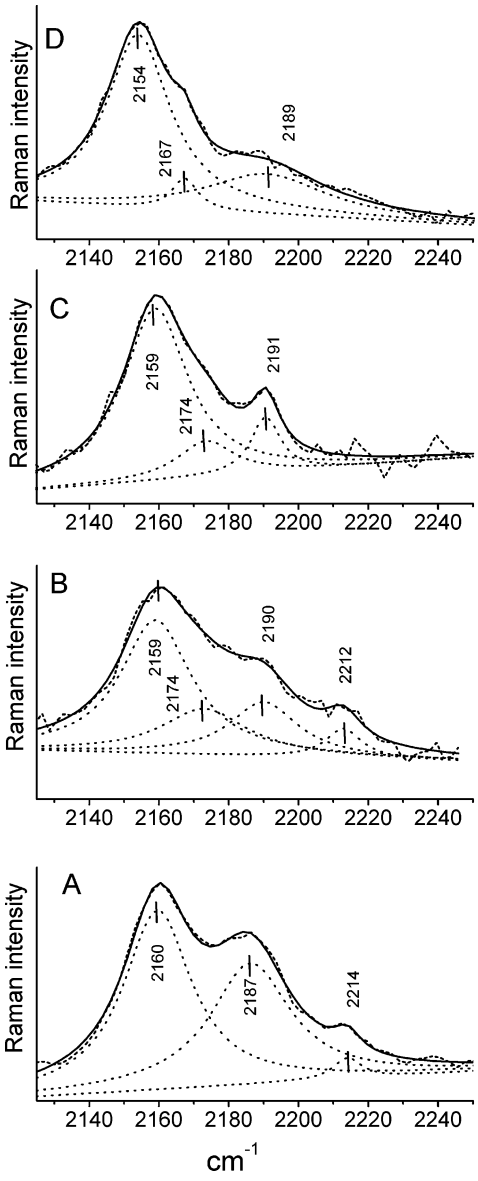

Figure 3. Band fitting of the C−D stretching region in the Raman spectra of HFIP-d_2 (20 mM) H-bonded with different amines as solvent. The component bands, whose peak positions are given, were determined by curve fitting assuming a linear combination of Lorentzian peaks. The dotted lines denote individual components, and the dashed lines the summations. The solid lines represent the experimentally determined spectra. Complexes with (A) *N*,*N*-dimethylaniline, (B) *N*-methylmorpholine, (C) *N*,*N*-diisopropylethylamine, and (D) triethylamine.

2212 cm^{-1} in *N*-methylmorpholine. These bands may be due to higher order associated aggregates.

HFIP-d_2 shows a band at ∼2105 ± 1 cm^{-1} (not shown in figure) which is absent in nonbasic solvents, e.g., chloroform, toluene, and CCl_4. The relative band intensity varied with amine and is attributed to the formation of an ammonium−alkoxide ion pair. A similar band is observed for ν_{C-D} on ionization of [1-D]trifluoroethanol[11] and HFIP-d_2 in aqueous 1 N NaOH, which has a single sharp ν_{C-D} at 2083 cm^{-1} assigned to the fully ionized alcohol.

The Raman spectra of HFIP-d_2 in the fingerprint region do not show remarkable changes when the molecules form H-bond complexes with amine solvents. This region of the Raman spectrum is obscured by many strong bands of the solvent making direct comparison to the chloroform−HFIP-d_2 spectrum difficult.

To eliminate the effect of the change in solvent and to permit direct comparison with the calorimetric results, the Raman spectra of HFIP-d_2−amine hydrogen-bonded complexes were determined in chloroform. The ν_{C-D} positions are recorded in Table 2 and shown in Figure 4. As in the spectra with the amines as solvent, the gauche and anti ν_{C-D} bands are red-shifted due to complex formation. Similar positions for ν_{C-D} were observed in the neat amine solvent and in the H-bonded complex in chloroform, indicating the effects were from H-bond formation and not changes in the solvent dielectric constant. Two qualitative observations are important: first, both ν_{C-D} features are red-shifted on H-bond formation; second, the separation between the two features decreases as the H-bond strength increases, i.e., the anti ν_{C-D} displays a greater red-shift than the gauche ν_{C-D}. H-bonding with quinuclidine, the strongest base (pK_a of 11.45), resulted in the maximum ν_{C-D} red-shift to 2153 and 2168 cm^{-1} for the gauche and anti conformations, respectively (Figure 4E), whereas with the weakest base, *N*,*N*-dimethylaniline, the corresponding band positions were at 2166 and 2192 cm^{-1} (Figure 4A). Bands originating from the uncomplexed monomer are also present in these systems (2191−2198 cm^{-1}). In *N*-methylmorpholine, a weak band at 2211 cm^{-1} was present and attributed to formation of a self-associated complex. The enthalpies of H-bond formation in chloroform were measured by isothermal titration calorimetry. The titration of HFIP with quinuclidine is shown in Figure 5. The enthalpy of H-bond formation between HFIP and the different amines varied from −2.0 kcal mol^{-1} with the weakest base, *N*,*N*-dimethylaniline, to −7.3 kcal mol^{-1} with the strongest base, quinuclidine. Intermediate values are listed in Table 2.

Figure 6 shows the variation of the HFIP-d_2 ν_{C-D} for both the gauche (panels A and B) and anti (panels C and D) conformers with the enthalpy of H-bond formation. By varying the amine acceptor, $-\Delta H_{H\text{-bond}}$ was systematically increased. The changes were determined either with the amine present in chloroform solution (panels A and C) or as the solvent (panels B and D). As anticipated, H-bond formation results in significant red-shifts in ν_{C-D}, and the magnitude of the red-shift is correlated with the H-bond strength. The effect of H-bond formation on the anti ν_{C-D} is greater than on the gauche ν_{C-D}

TABLE 2: Correlation of ΔH of H-Bond Formation with ν_{C-D} for HFIP-d_2 with Amine Bases[a]

base	K (M^{-1})	ΔH (kcal/mol)	ΔS (cal/mol/°)	pK_a	gauche ν_{C-D} (cm^{-1})	anti ν_{C-D} (cm^{-1})
chloroform					2168	2195
N,*N*-dimethylaniline	3	−2.0	−3	6.6	2166	2192
N-methyl morpholine	43	−3.3	−3	7.67	2158	2172
N,*N*−diisopropylethylamine	33	−6.4	−15	∼11.0	2161	2174
Triethylamine	90	−6.5	−6	11.2	2155	2164
Quinuclidine	298	−7.4	−13	11.45	2153	2168

[a] 20 mM HFIP-d_2 in the presence of 500 mM base in $CHCl_3$.

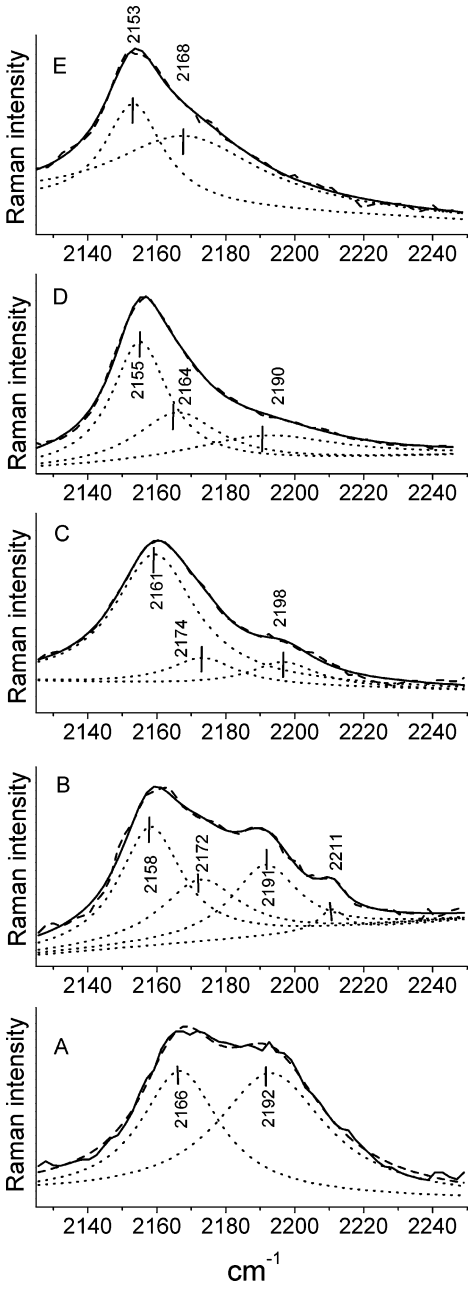

Figure 4. Band fitting of the C−D stretching region in the Raman spectra of HFIP-d_2 (20 mM) H-bonded with different amines (500 mM) in chloroform. The component bands, whose peak positions are given in the figure, were determined by curve fitting the spectra assuming a linear combination of Lorentzian peaks. The dotted lines denote individual components, and the dashed lines denote the sum of the functions. The solid lines represent the experimentally determined spectra. H-bonded complexes with (A) *N*,*N*-dimethylaniline, (B) *N*-methylmorpholine, (C) *N*,*N*-diisopropylethylamine, (D) triethylamine, and (E) quinuclidine.

as reflected in the greater slopes in panels C and D than observed in panels A and B.

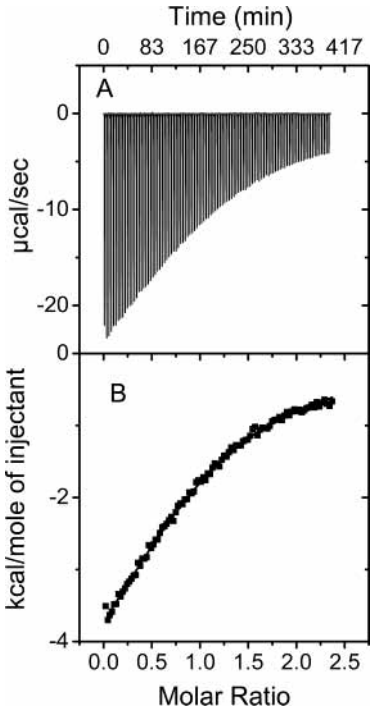

Figure 5. Isothermal calorimetric titration of HFIP (5 mM) in chloroform against quinuclidine (100 mM) in chloroform. (A) The recorded change in heat is shown (in units of μcal s^{-1}) as a function of time for successive injection of the base. (B) Integrated heats (black squares) plotted against the molar ratio of the association processes. The continuous line represents the results of nonlinear least-squares fitting of the data to a single site binding model.

Figure 7 shows a qualitative correlation between the gauche (panels A and B) and anti (panels C and D) ν_{C-D} features of HFIP-d_2 and the pK_a of the varied amine solvents. The correlations between ν_{C-D} and the pK_a of the amine solvents were very similar to the correlation with $-\Delta H_{H\text{-bond}}$. *N*,*N*-Diisopropylethylamine is a sterically hindered base with the branched isopropyl groups which have a minimal effect on the pK_a but which hinder formation of the H-bonded complex with HFIP, resulting in the diminished red-shift of ν_{C-D} observed with this amine. Density functional theory calculations, using the B3LYP hybrid functional[19] and a 6-31+G(d,p) basis set as implemented in Gaussian 98,[20] were used to predict the structure and Raman spectra of HFIP/HFIP-d_2 in its monomeric and H-bonded (trimethylamine) forms. Figure 8 shows the schematic presentation of the optimized structure of the gauche and anti conformers complexed with trimethylamine. Table 3 reports the calculated ν_{C-H}, ν_{C-D}, ν_{O-H}, and ν_{O-D} modes and the relative energetic contributions of the gauche and anti conformers.

Discussion

HFIP provides a well-characterized model system for investigating the spectroscopic effects of H bonds. Early studies characterized the existence of anti and gauche conformers (see

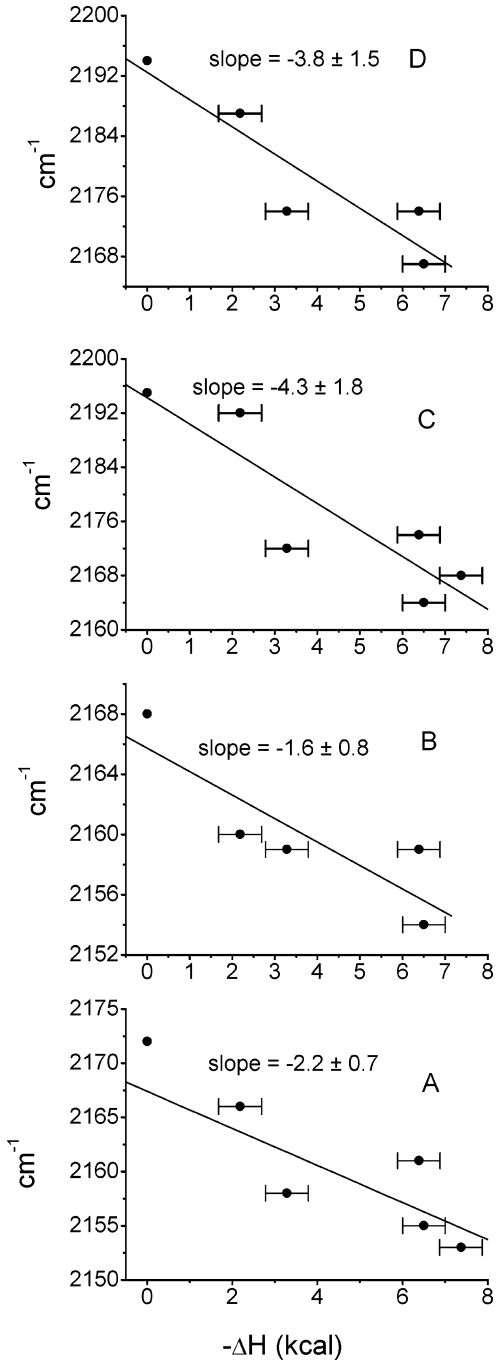

Figure 6. Plots of gauche and anti ν_{C-D} vs $-\Delta H$ for H-bond formation with HFIP-d_2. Linear regression results in the slopes indicated on the figures. (A) gauche ν_{C-D} vs $-\Delta H$ for H-bond formation in chloroform (intercept = 2169 ± 3; correlation coefficient = −0.83). (B) gauche ν_{C-D} in neat amine solvent vs $-\Delta H$ for H-bond formation in chloroform (intercept = 2165 ± 3; correlation coefficient = −0.74). (C) anti ν_{C-D} vs $-\Delta H$ for H-bond formation in chloroform (intercept = 2193 ± 7; correlation coefficient = −0.82). (D) anti ν_{C-D} in neat amine solvent vs $-\Delta$H for H-bond formation in chloroform (intercept = 2191 ± 6; correlation coefficient = −0.82).

Scheme 1) with different O−H(D) and C−H(D) stretching frequencies[12−15] and the existence of dimers in both condensed and gas phases. The significant difference in the spectroscopic properties of the anti and gauche conformers has been attributed to enhanced hyperconjugation of the C−H(D) bond when a nonbonding O electron pair is anti to the C−H(D) bond.[16,21,22] Although H-bonded complexes of HFIP with a broad range of acceptors have been investigated both experimentally[7] and with density functional theory calculations,[17] the potential for systematic effects of the H-bonding on the extent of the hyperconjugation and, consequently, on the ν_{C-H} has not been considered.

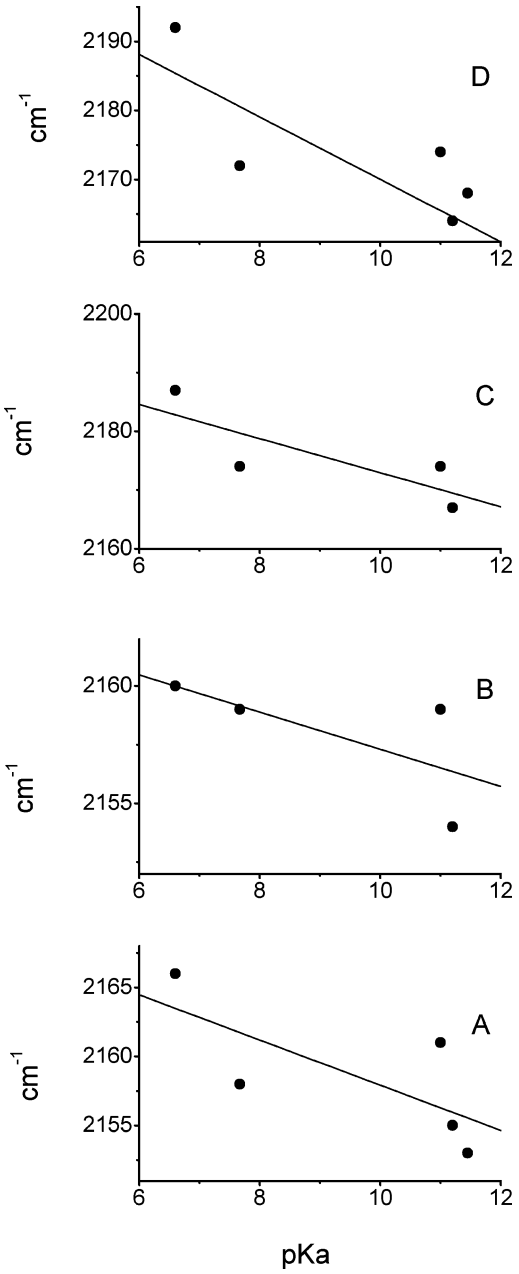

Figure 7. Variation of the ν_{C-D} stretching frequencies of the gauche and anti conformers of HFIP-d_2 acting as H-bond donors vs the pK_a of the amine acceptors. The regression lines indicate the qualitative trend. (A) gauche conformer of HFIP-d_2 H-bonded to amines in chloroform, (B) gauche conformer of HFIP-d_2 in neat amine solvents, (C) anti conformer of HFIP-d_2 H-bonded to amines in chloroform, and (D) anti conformer of HFIP-d_2 in neat amine solvents.

Initial calculations suggested that there should be a decrease in ν_{C-D} for the αC−D bond in alcohols as the strength of the O−H···acceptor H bond increases.[11] This effect was attributed to an enhanced negative hyperconjugation resulting from a delocalization of the electrons in the donor O−H bond. HFIP-d_2 was chosen as a model system to experimentally test this prediction because its acidity (pK_a = 9.3)[24] permitted a large range of acceptors to be considered and because its ν_{C-D} feature is in a spectroscopic "window" and can be characterized for both anti and gauche conformations.[17] As shown in Figure 3,

TABLE 3: Calculation of the αC−H Stretching Frequencies of HFIP[a] and Its H-Bonded Complexes[a,b]

	HFIP		HFIP-trimethylamine	
	anti	gauche	anti	gauche
E (Hartrees)	−789.84602	−789.84420	−964.35693	−964.35651
$\nu_{\alpha C-H\,(D)}$ (cm^{-1})	3120 (2300)	3053 (2248)	3081 (2269)	3040 (2238)
$\mu_{C-H(D)}$ amu	1.087 (2.345)	1.085 (2.333)	1.085 (2.335)	1.084 (2.335)
Raman activity	69 (34)	73 (36)	77	33
depolarization ratio	0.26	0.22	0.21	0.56
$\nu_{O-H\,(D)}$ (cm^{-1})	3789 (2759)	3829 (2789)	2895 (2134)	2932 (2163)
μ (O−H) amu	1.0063	1.0069	1.0797	1.0713
Raman activity	43 (22)	67 (46)	79	41
depolarization ratio	0.18	0.22	0.70	0.66

[a] Values for HFIP-d_2 listed in parentheses [b] Gas-phase calculation of complexes with trimethylamine at the B3LYP/6-31+G(d,p) level.

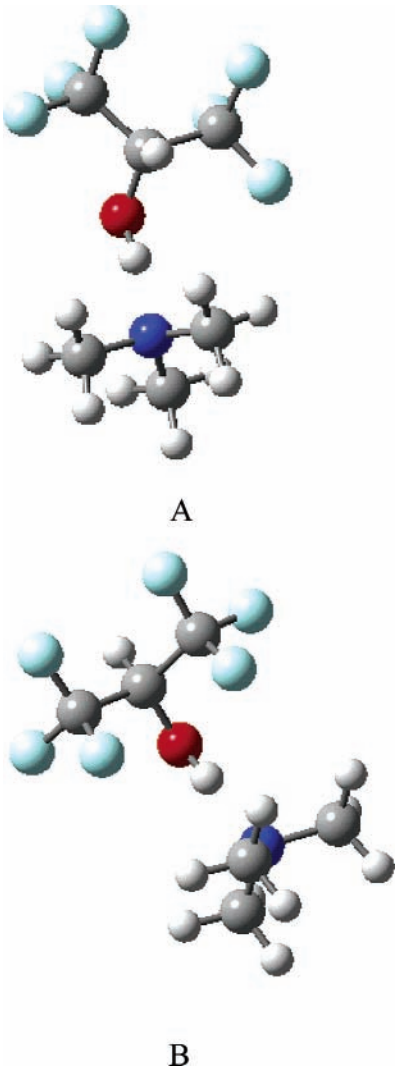

Figure 8. Ball and stick models of the energy minimized H-bonded complexes of HFIP. (A) gauche HFIP-TMA and (B) anti HFIP-TMA. The H-bond from HFIP is directed forward to the acceptor. Hydrogens are smaller balls and fluorine, carbon, oxygen, and nitrogen are depicted with an increasing gray scale.

the qualitative expectations were born out, and the correlations shown in Figures 6 and 7 are able to confirm two important trends, that stronger H-bonds generate greater red-shifts in ν_{C-D} and the effect of H-bonding is greater on ν_{C-D} for the anti conformation. As the H-bond strength increases, the O−H bond strength decreases and the electronic distribution becomes more and more symmetric; that is, the differences between the electronic environments of the anti and gauche C−H bonds diminishes. At the limit of complete ionization, the alkoxide is completely symmetrical and there will be no difference between the two conformers, as observed in 1 N NaOH.

Some of the deviation from linearity in Figures 6 and 7 is due to experimental error and the difficulties in identifying Raman maxima for the gauche and anti conformers as the resolution between the two features decreases. Figure 8 provides an additional suggestion as to why the correlation of ν_{C-D} with $\Delta H_{H\,bond}$ deviates from linearity. In the monomer, the B3LYP/6-31+G(d,p) optimized structures, as shown previously, have classical H−C−O−H torsion angles of −180 and +53° for the anti and gauche conformers, respectively. In the H-bonded case for the anti conformation, the torsion angle remains near 180°, but the gauche conformer is nearly eclipsed (H−C−O−H torsion angle of 19°). Negative hyperconjugation is greatest at ±60°, so any variation that occurs to accommodate H-bond formation would reduce the observed effect. This steric effect may be most pronounced for *N*,*N*-diisopropylethylamine which shows the greatest deviation from the linear correlation.

HFIP-d_2 in dilute chloroform solution has equal intensity features for both the gauche and anti conformations. Calculated Raman activities (Table 3) for C−H(D) stretches were nearly identical for the anti and gauche conformations. The anti conformer is stabilized by 1.1 kcal mol^{-1} relative to the gauche conformation in the gas-phase calculation, consistent with the experimental observation of 1 ± 0.25 kcal mol^{-1}.[25] The energy difference decreases to <0.1 kcal mol^{-1} in CCl_4.[17,26] In the H-bonded complexes, the lower frequency feature attributed to the gauche ν_{C-D} becomes relatively more intense, suggesting that either the Raman activity for this conformer is greater when present in a H-bond complex or H-bond formation with this conformer is preferred, or both. The gauche conformer will be a better H-bond donor as the lone electron pair formed on proton transfer will be anti to a CF_3 group. In the HFIP-trimethylamine complexes shown in Figure 8, the calculations indicate that the difference in energy between the gauche and anti conformations is decreased, consistent with the continued observation of ν_{C-D} features from both conformations.

We have attributed the band at 2105 cm^{-1} to formation of an intimate ion pair based on its presence in all solutions of HFIP-d_2 in amine solvents, varying by under ±1 cm^{-1}, and its complete absence in chloroform and toluene. Gawlita et al. also observed a similar red-shifted band for the ν_{C-D} of [1-D]-trifluoroethanol in NaOH solution.[11] Fermi resonance or overtone bands provide potential alternative interpretations of this feature but have been discounted. For Fermi resonance, a fundamental vibration must be close to the frequency of some overtone or combination mode. In the fingerprint region of the spectra, we found no vibrational modes around 1050 cm^{-1} whose first overtone band would be close to the ν_{C-D} for effective Fermi coupling.

Summary

The αC−D bond of HFIP, as a model of secondary and primary alcohols, has been shown to reflect the H-bonding interactions of the vicinal O−H function. The ν_{C-D} varies by over 100 cm^{-1}, from ∼2225 to 2105 cm^{-1}. The higher frequencies correspond to the HFIP-d_2 accepting an H bond. Vibrational frequencies below 2180 cm^{-1} are associated with HFIP-d_2 functioning as an H-bond donor and at ∼2105 cm^{-1} with the formation of an ion pair. For HFIP-d_2 acting as an H-bond donor, the correlation of the ν_{C-D} with the strength of the H bond is complicated by the presence of both gauche and anti conformer populations, but consistent with density functional calculations, the difference in ν_{C-D} between the two conformers decreases as the H-bond strength increases and there is a significant trend toward greater red-shifted ν_{C-D} with stronger H bonding. This experimental variation permits the αC−D bond to be a vicarious reporter of the H-bonding environment of alcohols in biomacromolecular complexes where specific labeling of the H-bond itself is not feasible.

Acknowledgment. This work was supported by grants from the National Science Foundation (MCB 0110610) and by NIH for acquisition of the isothermal titration calorimeter. We thank Dr. Jian Dong for his valuable assistance in operating the Raman spectrometer.

Supporting Information Available: Calculated bond lengths and angles for the optimized structure of HFIP (anti and gauche conformation) and their complexes (Table S1). Calculated bond lengths and angles for the optimized structure of HFIP(anti)−HFIP(gauche) dimer (Table S2). This material is available free of charge via the Internet at http://pubs.acs.org.

References and Notes

(1) Hibbert, F.; Emsley, J. Hydrogen bonding and chemical reactivity. In *Adv. Phys. Org. Chem.*; Bethell, D., Ed.; Academic Press: New York, 1990; Vol. 26, pp 255−379.

(2) Fersht, A. *Enzyme Structure and Mechanism*, 2nd ed.; W. H. Freeman and Company: New York, 1985.

(3) Mikenda, W. *J. Mol. Struct.* **1986**, *147*, 1−15.

(4) Mikenda, W.; Steinboeck, S. *J. Mol. Struct.* **1996**, *384*, 159−163.

(5) Perrin, C. L.; Nielson, J. B. *Annu. Rev. Phys. Chem.* **1997**, *48*, 511−44.

(6) Piaggio, P.; Tubino, R.; Dellepiane, C. *J. Mol. Struct.* **1983**, *96*, 277.

(7) Purcell, K. F.; Stikeleather, J. A.; Brunk, S. D. *J. Am. Chem. Soc.* **1969**, *91*, 4019−27.

(8) Tonge, P. J.; Carey, P. R. *Biochemistry* **1990**, *29*, 10723−10727.

(9) Tonge, P. J.; Carey, P. R. *Biochemistry* **1992**, *31*, 9122−9125.

(10) Deng, H.; Zheng, J.; Sloan, D.; Burgner, J.; Callender, R. *Biochemistry* **1992**, *31*, 5085−5092.

(11) Gawlita, E.; Lantz, M.; Paneth, P.; Bell, A.; Tonge, P.; Anderson, V. E. *J. Am. Chem. Soc.* **2000**, *122*, 11660−11669.

(12) Murto, J.; Kivinen, A.; Vitala, R.; Hyomaki, J. *Spectrochim. Acta, Part A: Mol. Biomol. Spectrosc.* **1973**, *29*, 1121−37.

(13) Kivinen, A.; Murto, J. *Suomen Kemistilehti B* **1967**, *40*, 6−13.

(14) Kivinen, A.; Murto, J.; Kilpi, L. *Suomen Kemistilehti B* **1969**, *42*, 19−28.

(15) Kivinen, A.; Murto, J.; Liljequist, S.; Vaara, S. *Acta Chem. Scand., Ser. A: Phys. Inorg. Chem.* **1975**, *A29*, 911−18.

(16) Krueger, P. J.; Jan, J.; Wieser, H. *J. Mol. Struct.* **1970**, *5*, 375−387.

(17) Schaal, H.; Haeber, T.; Suhm, M. A. *J. Phys. Chem. A* **2000**, *104*, 265−274.

(18) Dong, J.; Dinakarpandian, D.; Carey, P. R. *Appl. Spectrosc.* **1998**, *52*, 1117−1122.

(19) Becke, A. D. *J. Chem. Phys.* **1993**, *98*, 5648.

(20) Frisch, M. J.; Trucks, G. W.; Schlegel, H. B.; Scuseria, G. E.; Robb, M. A.; Cheeseman, J. R.; Zakrzewski, V. G.; Montgomery, J. A., Jr.; Stratmann, R. E.; Burant, J. C.; Dapprich, S.; Millam, J. M.; Daniels, A. D.; Kudin, K. N.; Strain, M. C.; Farkas, O.; Tomasi, J.; Barone, V.; Cossi, M.; Cammi, R.; Mennucci, B.; Pomelli, C.; Adamo, C.; Clifford, S.; Ochterski, J.; Petersson, G. A.; Ayala, P. Y.; Cui, Q.; Morokuma, K.; Malick, D. K.; Rabuck, A. D.; Raghavachari, K.; Foresman, J. B.; Cioslowski, J.; Ortiz, J. V.; Stefanov, B. B.; Liu, G.; Liashenko, A.; Piskorz, P.; Komaromi, I.; Gomperts, R.; Martin, R. L.; Fox, D. J.; Keith, T.; Al-Laham, M. A.; Peng, C. Y.; Nanayakkara, A.; Gonzalez, C.; Challacombe, M.; Gill, P. M. W.; Johnson, B. G.; Chen, W.; Wong, M. W.; Andres, J. L.; Head-Gordon, M.; Replogle, E. S.; Pople, J. A. *Gaussian 98*, revision A.3; Gaussian, Inc.: Pittsburgh, PA, 1998.

(21) DeFrees, D. J.; Taagepera, M.; Levi, B. A.; Pollack, S. K.; Summerhays, K. D.; Taft, R. W.; Wolfsberg, M.; Hehre, W. J. *J. Am. Chem. Soc.* **1979**, *101*, 5532−5536.

(22) Williams, I. H. *THEOCHEM* **1983**, *14*, 105−17.

(23) Badger, R. M.; Bauer, S. H. *J. Chem. Phys.* **1937**, *5*, 839−51.

(24) Middleton, W. J.; Lindsey, R. V., Jr. *J. Am. Chem. Soc.* **1964**, *86*, 4948−52.

(25) Quack, M. *J. Chem. Soc., Faraday Trans.* **1995**, *102*, 104−107.

(26) Murto, J.; Kivinen, A. *Suomen Kemistilehti B* **1967**, *40*, 14−18.